Electronic Supplementary Information

Stabilization of Grignard reagents by a pillar[5]arene host – Schlenk equilibria and Grignard reactions

Lingyi Shen,[a] Yanxia Zhao,[a] Dihua Dai,[b] Ying-Wei Yang,*[b] Biao Wu[a,c] and Xiao-Juan Yang*[a]

Table of Contents

S1. Experimental section

General information. All the reactions and manipulations of air- and moisture-sensitive compounds were carried out under argon or nitrogen with standard Schlenk or drybox techniques. The solvent toluene was refluxed over sodium and was distilled under argon prior to use. Benzene-d_6 was dried over Na/K alloy. DMpillar[5]arene was prepared according to literature procedures.[1] Grignard reagents (in THF solution) were purchased from Aladdin. Potassium metal was purchased from Alfa Aesar. NMR spectra were recorded on a Bruker Avance III-400 MHz NMR spectrometer in benzene-d_6.

Synthesis of host-guest complex 1: The solvent THF (0.5 M in THF, ca. 2.0 mmol) in a 4.0 mL *n*-BuMgBr solution was removed under vacuum, and a neat toluene (15 mL) solution of P5A (0.375 g, 0.5 mmol) was added. After stirring for 12 h the resulting mixture was filtered and the filtrate was concentrated. Slow evaporation of the toluene solution afforded colorless crystals in two weeks (0.35 g, 59% based on P5A). ^{1}H NMR (400 MHz, C_6D_6, 298 K): δ 0.05 (t, 6H, *n*-butyl-CH_2, J = 8.4 Hz), 1.19 (t, 9H, *n*-butyl-CH_3, J = 7.2 Hz), 1.71 (m, 6H, *n*-butyl-CH_2), 1.96 (m, 6H, *n*-butyl-CH_2), 1.02 (m, 8H, THF-CH_2), 3.53 (m, 8H, THF-CH_2), 3.33 (s, 30H, P5A-OCH_3), 4.11 (s, 10H, P5A-CH_2), 6.83 (s, 10H, P5A-Ar-*H*) ppm. ^{13}C NMR (100.6 MHz, C_6D_6): *n*-butyl: δ = 8.8, 14.9, 32.1, 32.6; THF: δ = 25.3, 69.8; P5A: δ = 30.9, 56.7, 115.4, 129.8, 151.9 ppm.

Synthesis of 2: The solvent THF of 4 mL *n*-BuMgBr solution (0.5 M in THF, ca. 2.0 mmol) was removed under vacuum, and a neat toluene (15 mL) solution of P5A (0.375 g, 0.5 mmol) and potassium metal (0.098 g, 2.5 mmol) were added. After stirring for 12 h the resulting mixture was filtered and the filtrate was concentrated. Colorless crystals were grown from the solution in two weeks (0.33 g, 56%). ^{1}H NMR (400 MHz, C_6D_6, 298 K): δ 0.02 (t, 7.2H, *n*-butyl-CH_2, J = 8.4 Hz), 1.20 (t, 10.8H, *n*-butyl-CH_3, J = 7.2 Hz), 1.71 (m, 7.2H, *n*-butyl-CH_2), 1.94 (m, 7.2H, *n*-butyl-CH_2), 1.10 (m, 8H, THF-CH_2), 3.55 (m, 8H, THF-CH_2), 3.30 (s, 30H, P5A-OCH_3), 4.12 (s, 10H, P5A-CH_2), 6.81 (s, 10H, P5A-Ar-*H*) ppm. ^{13}C NMR (100.6 MHz, C_6D_6): *n*-butyl: δ = 9.1, 14.9, 32.3, 32.4; THF: δ = 25.4, 69.6; P5A: δ = 31.0, 56.4, 115.1, 129.7, 152.1 ppm.

Synthesis of 3: Complex **3** was prepared by a similar procedure to that employed for **2**, by reacting 0.5 mmol P5A with 1.0 mL *n*-BuMgCl (2.0 M in THF, 2.0 mmol) and K (0.098 g, 2.5 mmol), as colorless crystals (0.32 g, 55%). ^{1}H NMR (400 MHz, C_6D_6, 298 K): δ 0.02 (t, 8H, *n*-butyl-CH_2, J = 8.4 Hz), 1.17 (t, 12H, *n*-butyl-CH_3, J = 7.2 Hz), 1.71 (m, 8H, *n*-butyl-CH_2), 1.90 (m, 7.2H, *n*-butyl-CH_2), 1.04 (m, 8H, THF-CH_2), 3.55 (m, 8H, THF-CH_2), 3.32 (s, 30H, P5A-OCH_3), 4.11 (s, 10H, P5A-CH_2), 6.83 (s, 10H, P5A-Ar-*H*) ppm. ^{13}C NMR (100.6 MHz, C_6D_6): *n*-butyl: 9.1, 14.9, 32.2, 32.4; THF: 25.3, 69.6; P5A: 30.9, 56.5, 115.3, 129.7, 151.4 ppm.

Synthesis of 4: Complex **4** was prepared by a similar procedure from 0.5 mmol P5A, (*n*-pentyl)MgBr (1.0 M in THF, 2.0 mmol), and K (0.098 g, 2.5 mmol) as colorless crystals (0.31 g, 50%). ^{1}H NMR (400 MHz, C_6D_6, 298 K): δ 0.01 (t, 8H, *n*-pentyl-CH_2, J = 8.4 Hz), 1.07 (t, 12H, *n*-pentyl-CH_3, J = 7.2 Hz), 1.56−1.66 (m, 16H, *n*-pentyl-CH_2), 1.96 (m, 8H, *n*-pentyl-CH_2), 1.14 (m, 8H, THF-CH_2), 3.56 (m, 8H, THF-CH_2), 3.30 (s, 30H, P5A-OCH_3), 4.12 (s, 10H, P5A-CH_2), 6.81 (s, 10H, P5A-Ar-*H*) ppm. ^{13}C NMR (100.6 MHz, C_6D_6): *n*-pentyl: 9.4, 14.9, 23.6, 29.3, 42.0; THF: 25.5, 69.8; P5A: 31.2, 56.2, 115.0, 130.0, 152.0 ppm.

Synthesis of 5: Complex **5** was prepared by a similar procedure from 0.5 mmol P5A, (*n*-heptyl)MgBr (1.0 M in THF, 2.0 mmol), and K (0.098 g, 2.5 mmol) as colorless crystals (0.34 g, 65%). ^{1}H NMR (400 MHz, C_6D_6, 298 K): δ 0.01 (t, 4H, *n*-heptyl-CH_2, J = 8.4 Hz), 0.93 (t, 6H, *n*-heptyl-CH_3, J = 7.2 Hz), 1.33−1.49 (m, 8H, *n*-heptyl-CH_2), 1.61 (m, 4H, *n*-heptyl-CH_2), 1.72 (m, 4H, *n*-heptyl-CH_2), 2.00 (m, 4H,

n-heptyl-CH_2); 1.16 (m, 8H, THF-CH_2), 3.56 (m, 8H, THF-CH_2), 3.31 (s, 30H, P5A-OCH_3), 4.15 (s, 10H, P5A-CH_2), 6.82 (s, 10H, P5A-Ar-*H*) ppm. ^{13}C NMR (100.6 MHz, C_6D_6): *n*-pentyl: 9.6, 14.8, 23.7, 29.3, 30.5, 33.2, 39.8; THF: 25.5, 69.3; P5A: 31.1, 56.2, 115.1, 129.6, 151.9 ppm.

Synthesis of 6: Complex **6** was prepared by a similar procedure from 0.5 mmol P5A, (*n*-octyl)MgBr (1.0 M in THF, 2.0 mmol) as colorless crystals (0.39 g, 70%). ^{1}H NMR (400 MHz, C_6D_6, 298 K): δ 0.10 (t, 2H, *n*-octyl-CH_2, J = 8.0 Hz), 0.81 (t, 3H, *n*-octyl-CH_3, J = 7.2 Hz), 1.18 (m, 4H, *n*-octyl-CH_2), 1.40 (m, 2H, *n*-octyl-CH_2), 1.58 (m, 2H, *n*-octyl-CH_2), 1.74 (m, 2H, *n*-octyl-CH_2), 2.07 (m, 2H, *n*-octyl-CH_2); 1.00 (m, 8H, THF-CH_2), 3.56 (m, 8H, THF-CH_2), 3.38 (s, 30H, P5A-OCH_3), 4.14 (s, 10H, P5A-CH_2), 6.90 (s, 10H, P5A-Ar-*H*) ppm. ^{13}C NMR (100.6 MHz, C_6D_6): *n*-pentyl: δ = 8.7, 14.8, 23.5, 30.7, 30.8, 30.9, 33.0, 39.8; THF: δ = 25.3, 69.6; P5A: δ = 30.9, 56.3, 115.0, 129.6, 151.8 ppm.

S2. X-ray Crystallographic Analysis

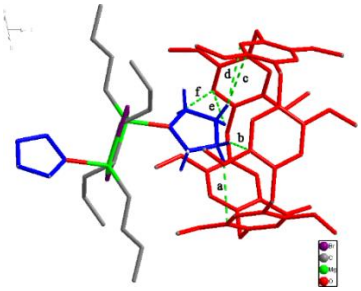

Fig. S1. Part of the infinite structure of the host-guest complex **1**. P5A is in red, THF in blue. Hydrogen atoms involved in the C–H···π interactions are shown, while other hydrogen atoms and solvents are omitted for clarity. The green dotted lines indicate the C–H···π interactions (C–H ··π distances: a = 2.91, b = 3.01, c = 2.89, d = 2.83, e = 3.00, f = 2.90 Å).

In complex **1**, each THF molecule forms seven C–H···π interactions involving five hydrogen atoms and the central aryl rings of P5A with distances of 2.84–3.01 Å (Fig. S1), which are within the range of interatomic distance in a C–H···π interaction (up to 3.05 Å).[2] In the encapsulated free THF molecules, similar interactions were observed.[3] On the other hand, there is no C–H···O hydrogen bonding interaction between THF and the methoxy rims of P5A (the shortest H ··O distance, 2.77 Å, is longer than 2.72 Å of the sum of the van der Waals radii of hydrogen and oxygen atoms).[4]

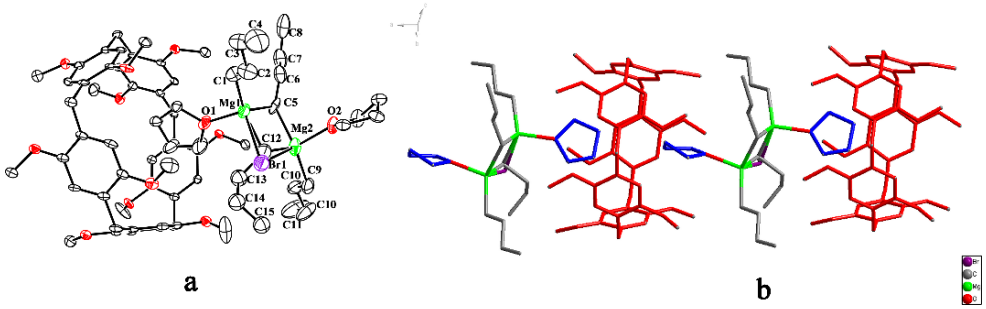

Fig. S2. Crystal structure of the host-guest complex **2**. **a**: Ortep representation showing the encapsulation of the coordinated THF molecule in the cavity of P5A (thermal ellipsoids are set at the 30% probability level; hydrogen atoms and free solvents are omitted for clarity). **b**: Part of the infinite 1D chain of **2**. Selected bond lengths (Å) and angles (°): Mg1 ··Mg2 2.848(4), Mg1−C1 2.119(11), Mg1−C5 2.375(9), Mg1−C13 2.04(2), Mg1−O1 2.042(7), Mg1−Br1 2.665(5), Mg2−C9 2.198(11), Mg2−C5 2.336(9), Mg2−C13 2.14(2), Mg2−O2 2.071(7), Mg2−Br1 2.564(5); C1−Mg1−C5 122.9(4), C5−Mg1−C13 100.6(6), C5−Mg2−C9 118.7(3), C5−Mg1−C13 100.6(6), Mg1−C5−Mg2 74.4(3), Mg1−C13−Mg2 86.0(8).

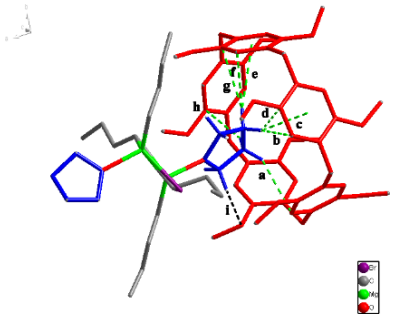

Fig. S3. Wire view of part of the infinite chain of complex **2**, showing the eight C–H···π interactions (green dotted lines) and one C–H···O (black dotted line) interaction between four hydrogens of THF and aryl planes of P5A. Only hydrogen atoms related to these interactions are preserved. C–H ··π distances (Å): a = 2.87, b = 2.89, c = 2.99, d = 2.87, e = 3.05, f = 2.98, g = 2.96, h = 2.87; C–H ··O distance (Å): i = 2.70, C–H…O angle (°): h = 123.

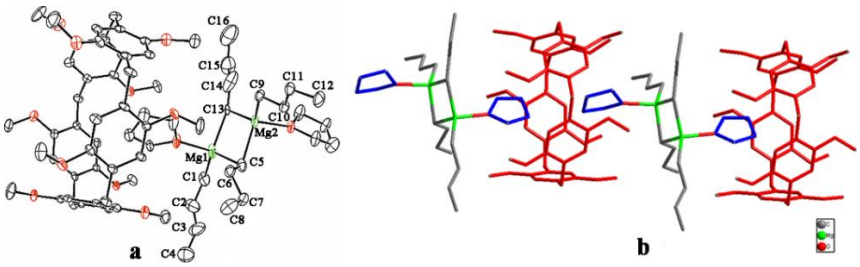

Fig. S4. Crystal structure of **3**. a) Ortep representation showing the encapsulation of the coordinated THF molecule in the cavity of P5A (thermal ellipsoids are set at the 30% probability level; hydrogen atoms and free solvents are omitted for clarity). b) Part of the infinite 1D chain of **3**. Selected bond lengths (Å): Mg1 ··Mg2 2.791(3), Mg1−C1 2.136(6), Mg1−C5 2.264(7), Mg1−C13 2.347(6), Mg2−C9 2.140(5), Mg2−C13 2.324(5), Mg2−C5 2.300(7).

In complex **3**, the dibutylmagnesium shows a distorted tetrahedral arrangement around Mg atom, with one terminal and two bridging *n*Bu groups and a THF molecule. The bridging Mg1−C5 (2.264(7) Å) and Mg2−C5 (2.300(7) Å) bonds are quite long compared to the sum of the covalent radii [2.17 Å] of Mg and C atoms. However, they are close to the bridging Mg−C bonds in related complexes, $[\{(CH_3)_2Si(CH_2NC_5H_{10})(NR)\}Mg(n\text{-}Bu)]_2$ (2.276(3) Å),[5] $[^nBu_2Mg]_4 \cdot 2IPr$ (2.250(3) Å),[6] and [NN-(Mg*n*Bu)$_2$] (2.225(3) and 2.241(3) Å).[7] On the other hand, the terminal Mg1−C1 (2.136(6) Å) and Mg2−C9 (2.140(5) Å) bonds are slightly longer than those in mononuclear magnesium complexes, *n*BuMg(TMP) ·IPr (2.126(2) Å) and *n*BuMg(HMDS) ·IPr (2.140(2) Å; HMDS = 1,1,1,3,3,3-hexamethyldisilazide).[6]

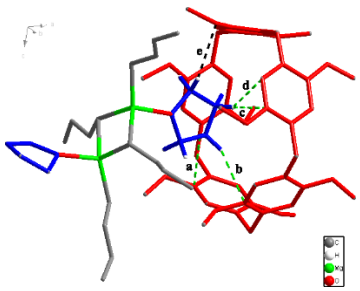

Fig. S5. Wire view of part of the infinite chain of complex **3**, showing the C–H···π (green dotted lines) and C−H···O (black dotted line) interaction. C–H ··π distances (Å): a = 2.92, b = 2.89, c = 3.01, d = 2.89; C–H ··O distance (Å): e = 2.65, C–H…O angle ( ): e = 126.

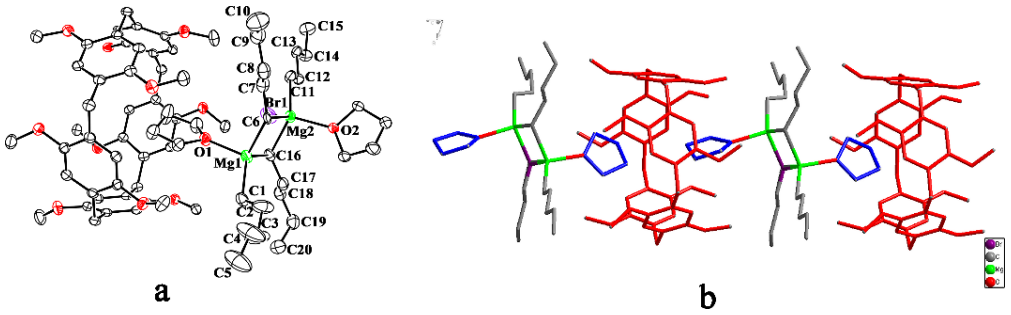

Fig. S6 Crystal structure of the host-guest complex **4**. **a**: Ortep representation showing the encapsulation of the coordinated THF molecule in the cavity of P5A. **b**: Part of the infinite 1D chain of **4**. Selected bond lengths (Å) and angles (°): Mg1 ··Mg2 2.7670(18), Mg1−C1 2.117(3), Mg1−C16 2.253(7), Mg1−O1 2.046(3), Mg2−O2 2.025(2), C11−Mg2 2.110(3), C16−Mg2 2.297(3); O1−Mg1−C1 110.05(12), C11−Mg2−C6 119.7(2), C11−Mg2−C16 113.74(13), O2−Mg2−C11 108.44(11), O2−Mg2−C16 106.52(11).

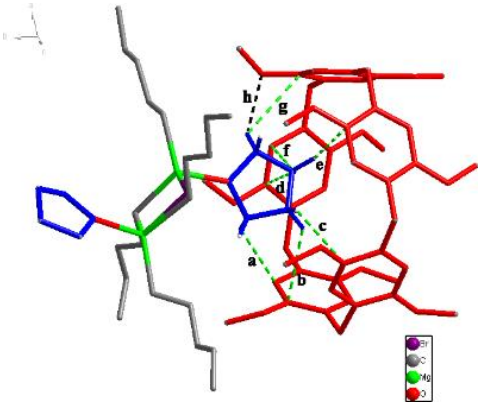

Fig. S7. Part of the infinite chain of complex **4**, showing the C–H···π (green dotted lines) and C−H···O (black dotted line) interactions. C–H ··π distances (Å): a = 3.03, b = 3.00, c = 2.84, d = 3.01, e = 2.93, f = 2.89, g = 3.03; C–H ··O distance (Å): h=2.59, C–H ··O angle (°): h = 147.

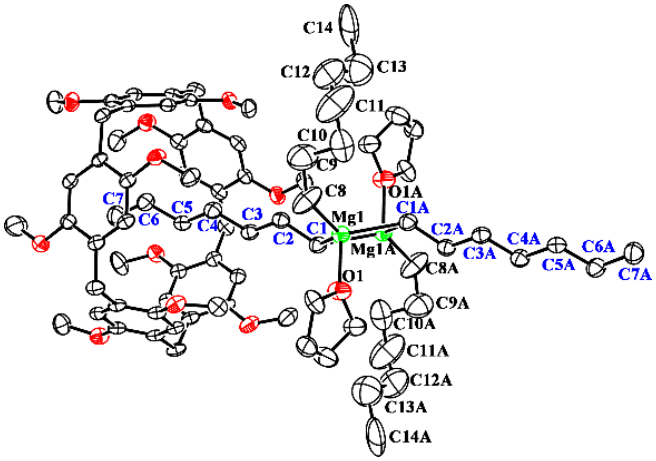

Fig. S8. Crystal structure of the host-guest complex **5**. Ortep representation showing the coordinated n-heptyl chain being encapsulated in the cavity of P5A (thermal ellipsoids are set at the 30% probability level; hydrogen atoms and free solvents are omitted for clarity). Selected bond lengths (Å) and angles (°): Mg1 ··Mg2 2.737(2), Mg1−C1 2.297(4), Mg1−O1 2.047(3), Mg1−C8 2.113(5); C1−Mg1−C8 121.2(2), C1−Mg1−C1A 106.60(13), O1−Mg1−C1 102.64(15), O1−Mg1−C1A 103.33(14), O1−Mg1−C8 100.84(19). Symmetry code: A, 1−*x*, −*y*, 1−*z*; A, 1−*x*, 2−*y*, 2−*z*.

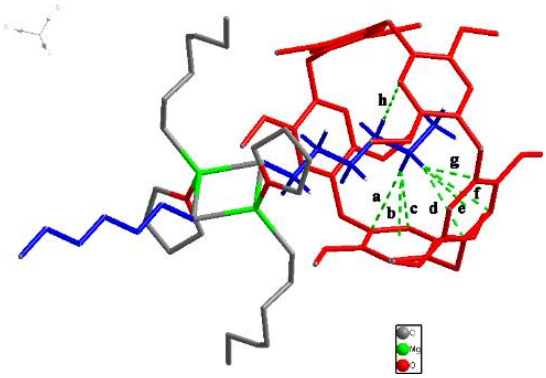

Fig. S9. Part of the dimeric structure of complex **5** (with one P5A molecule) showing the C–H···πinteractions (green dotted lines). C–H ··π distances (Å): a = 2.98, b = 2.80, c = 2.94, d = 3.04, e = 2.77, f = 2.93, g = 2.99, h = 2.96.

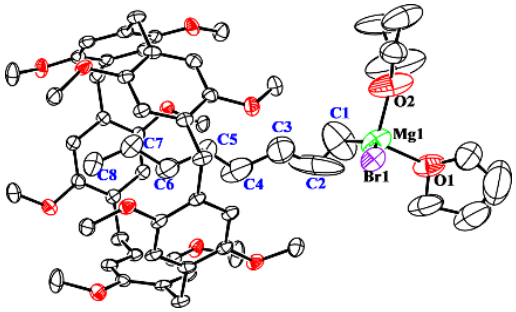

Fig. S10. Crystal structure of **6**. Ortep representation showing the coordinated *n*-octyl chain being encapsulated in the cavity of P5A (thermal ellipsoids are set at the 30% probability level; hydrogen atoms and free solvents are omitted for clarity) Selected bond lengths (Å) and angles (°): C1–Mg1 2.026(11); Mg1–O1 1.999(9); Mg1–O2 2.016(7); O1–Mg1–C1 94.5(5); O1–Mg1–O2 98.5(4).

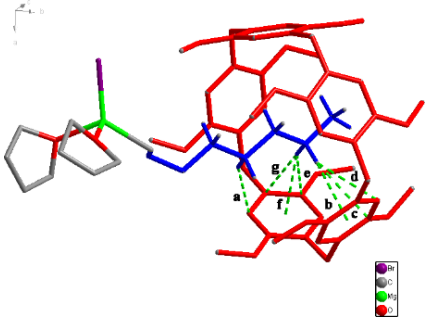

Fig. S11. Crystal structure of monomeric complex **6**. P5A is in red, *n*-octyl is in blue. The green dotted lines indicate the C–H···π interactions: a = 2.91, b = 2.80, c = 2.89, d = 2.98, e = 2.95, f = 2.80, g = 3.01 Å.

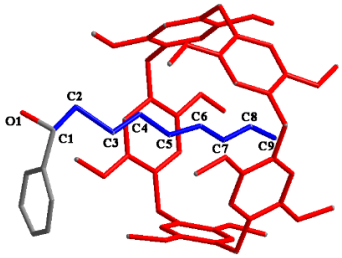

Fig. S12. Crystal structure of the inclusion complex 1-phenylnonan-1-ol⊂P5A (**7**).

X-ray crystal structure determination. X-ray diffraction data for compounds **1**−**3** were collected on a Bruker SMART APEX II diffractometer and the data of compounds **4**−**7** were collected on a Bruker D8 Venture photon II diffractometer at low temperature (150−153 K) with graphite-monochromated Mo Kα radiation (λ = 0.71073 Å). An empirical absorption correction using SADABS was applied for all data.[8] The structures were solved and refined to convergence on F^2 for all independent reflections by the full-matrix least squares method using the SHELXL−2014 programs[9] and OLEX2 1.2.[10] In complex **1**, one carbon atom in solvent THF was disordered into two positions. In complex **3**, there is a large amount of disorder in the structure, which caused the level B alerts. In particular the disordered side-chains are very dynamic and may be considered as a solvent. Short contacts between disordered fragments are to be expected. In complex **5**, about 1 THF molecule per formula (Z = 1) is co-crystallized, with the corresponding electron density (38 electrons) being removed using SQUEEZE,[11] and the resulting .fab file was processed with OLEX2 1.2 using the ABIN instruction. Moreover, a level B alert is caused by the alkyl-chain. In complex **6**, about 0.3 toluene molecule per formula (Z = 4) is co-crystallized, with the corresponding electron density (56 electrons) being removed using SQUEEZE,[11] and the resulting .fab file was processed with OLEX2 1.2 using the ABIN instruction. In addition, one THF molecule, two bromine atoms and a magnesium atom were disordered over two positions. Moreover, some atoms in the other THF solvent are disordered and display unusual thermal parameters, which caused the level B alerts. In addition, the last level B alert may occur with area detector data. Data completeness of is 99.8% which guarantees a correct structural elucidation of complex **6**. In complex **7**, 0.5 P5A molecule and one oxygen were disordered over two positions. We made several attempts to obtain better quality data for this structure however, due to twinning, disorder, poor crystal quality etc. the R_2 value is high. This structure was included for comparison with the other similar complexes and characterized by H1 NMR spectra. Moreover, data completeness of is 99.5% which guarantees a correct structural elucidation of complex **7**. We are confident the structural characterization is valid. and there is a large amount of disorder in the structure, which caused the level B alerts. Crystallographic data for complexes **1**–**7** are given in Table S1 and Table S2.

CCDC **1**–**3:** 1942603−1942605, **4**–**7:** 1942607–1942610 contain the supplementary crystallographic data for this paper. These data can be obtained free of charge from the Cambridge Crystallographic Data Centre www.ccdc.cam.ac.uk/data_request/cif

Table S1. Crystallographic data and refinement details for complexes **1**−**3**.

Complex	**1**	**2**	**3**
Formula	$C_{65.96}H_{95.17}Br_{0.76}Mg_2O_{12}$	$C_{67.57}H_{98.78}Br_{0.36}Mg_2O_{12}$	$C_{69}H_{102}Mg_2O_{12}$
Formula weight	1189.51	1180.46	1172.15
Crystal system, space group	Monoclinic *C2/c*	Monoclinic $P2_1$	Monoclinic $P\ 2_1/c$
a /Å	20.510(6)	13.565(3)	13.392(4)
b /Å	12.667(4)	12.450(3)	21.180(6)
c /Å	26.498(7)	20.554(4)	23.936(7)
α /deg	90	90	90
β /deg	108.671(4)	107.915(3)	96.985(4)
γ /deg	90	90	90
V /Å^3	6522(3)	3302.9(11)	6739(3)
Z	4	2	4
D_{calcd} /g cm^{-3}	1.211	1.187	1.154
F(000)	2550	1274	2540
μ /mm^{-1}	0.560	0.312	0.094
θ range	1.92−25.07	1.94−25.00	1.71−25.32

Independent reflections	5667	11320	12056
R_{int}	0.0531	0.0383	0.0795
Final R_1, wR_2 values *(I> 2σ(I))*	0.0876, 0.2462	0.0768, 0.2181	0.0976, 0.2524
R_1, wR_2 (all data)	0.1399, 0.2869	0.0996, 0.2354	0.1677, 0.3098
GOF (F^2)	1.044	1.059	1.029

Table S2. Crystallographic data and refinement details for complexes **4**−**7**.

Complex	**4**	**5**	**6**	**7**
Formula	$C_{72.34}H_{107.54}Br_{0.14}Mg_2O_{12}$	$C_{251.55}H_{351.03}Br_{0.06}Mg_4O_{44}$	$C_{122}H_{164}Br_2Mg_2O_{24}$	$C_{186}H_{228}O_{33}$
Formula weight	1228.54	4180.97	2223.01	2991.67
Crystal system	Triclinic	Triclinic	Monoclinic	Monoclinic
space group	*P*-1	*P*-1	$P2_1/c$	*C*2/c
a /Å	11.959(8)	14.0100(7)	11.973(5)	40.636(4)
b /Å	13.536(9)	17.8060(9)	26.293(12)	12.2639(10)
c /Å	22.775(13)	25.7096(13)	39.008(17)	36.165(3)
α /deg	75.943(17)	95.703(2)	90	90
β /deg	88.27(2)	103.750(2)	97.456(12)	113.845(3)
γ /deg	73.195(16)	102.801(2)	90	90
V /Å^3	3421(4)	5996.2(5)	12176(10)	16485(3)
Z	2	1	4	4
D_{calcd} /g cm^{-3}	1.193	1.158	1.213	1.205
F(000)	1333	2262	4732	6432
μ /mm^{-1}	0.174	0.098	0.743	0.081
θ range	2.14−25.24	1.65−25.06	2.13−25.00	2.337−25.02
Independent reflections	12260	21184	21391	14504
R(int)	0.0408	0.0650	0.0777	0.0740
Final R_1, wR_2 values *(I> 2σ(I))*	0.0656, 0.1697	0.0772, 0.2101	0.1035, 0.2816	0.1147, 0.3159
R_1, wR_2 (all data)	0.0815, 0.1826	0.1076, 0.2366	0.1591, 0.3414	0.1722, 0.3730
GOF (F^2)	1.039	1.035	1.014	1.130

S3. ^{1}H- and ^{13}C-NMR spectra of complexes 1−6.

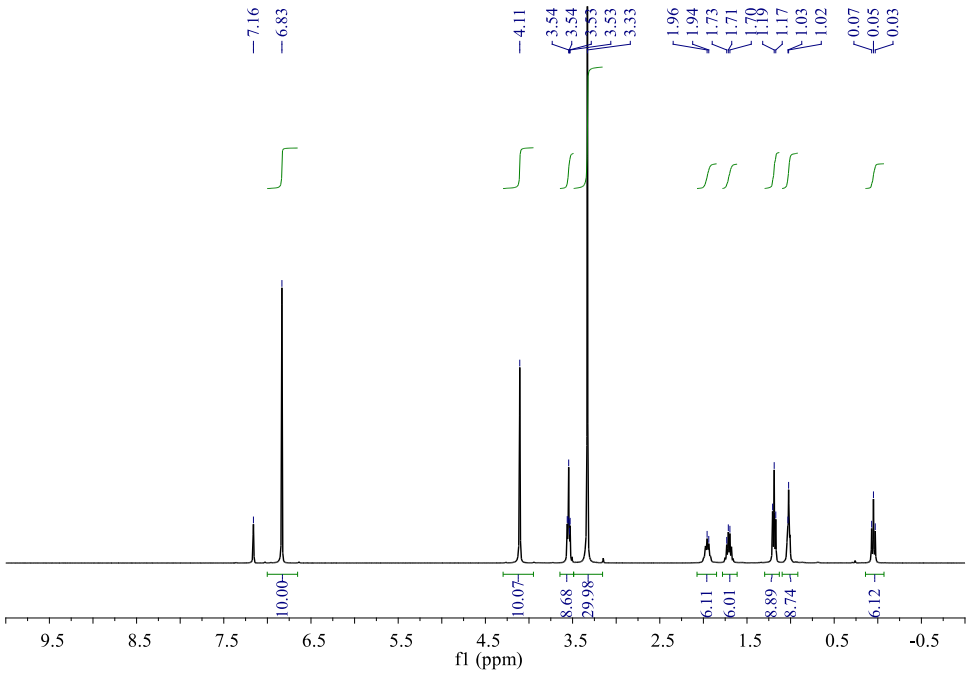

Fig. S13. ^{1}H NMR (400 MHz, C_6D_6, 298 K) of complex **1**.

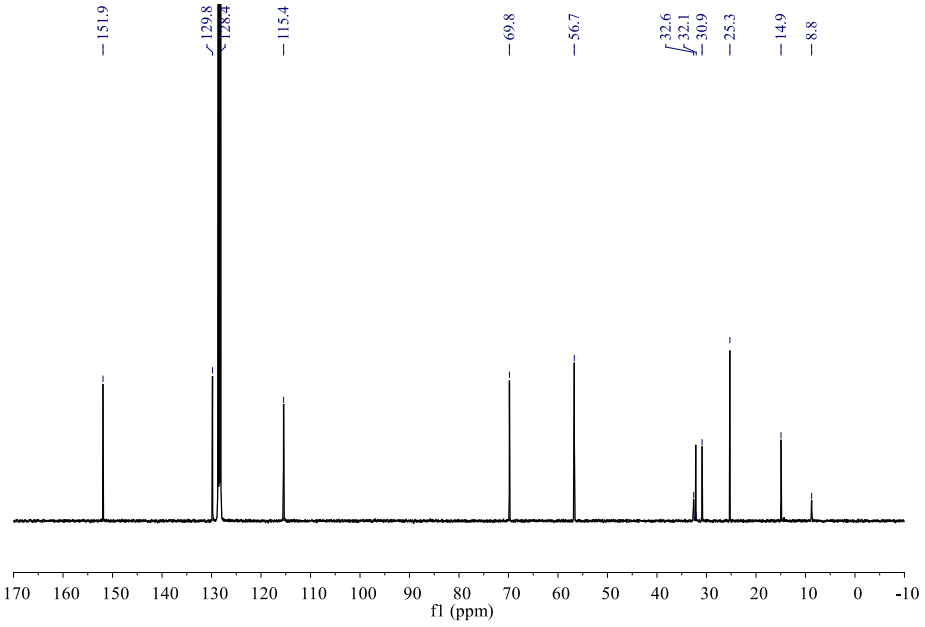

Fig. S14. ^{13}C NMR (100.6 MHz, C_6D_6, 298 K) of complex **1**.

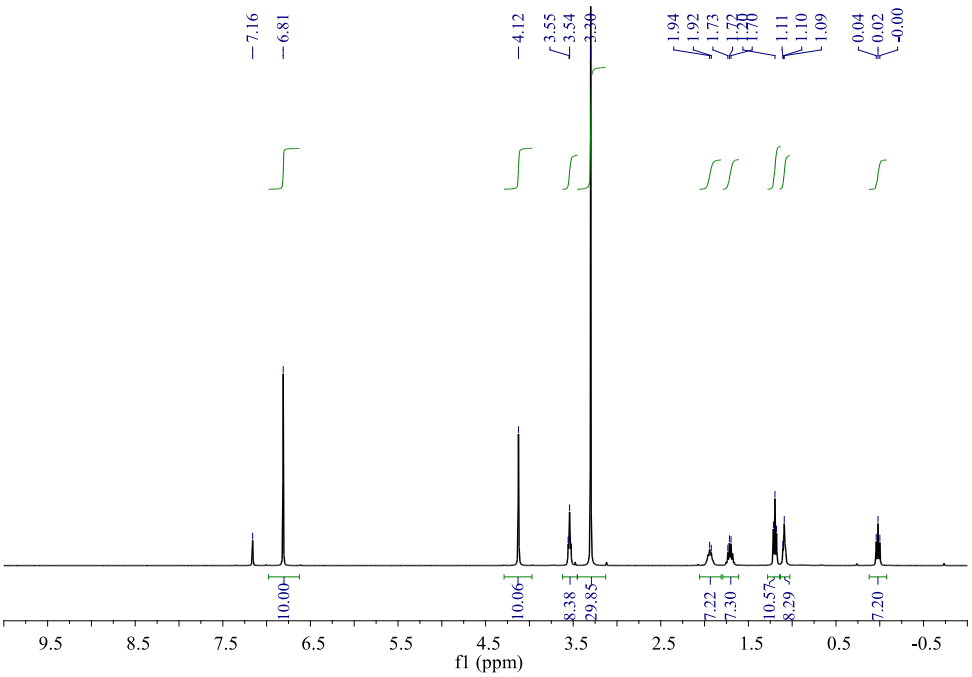

Fig. S15. ^{1}H NMR (400 MHz, C_6D_6, 298 K) of complex **2**.

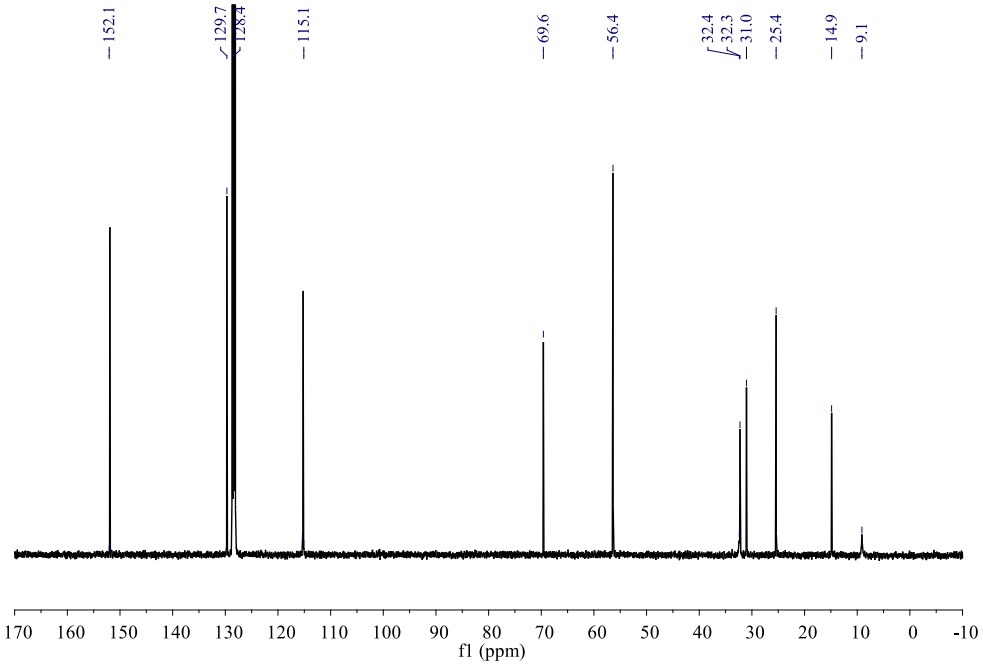

Fig. S16. ^{13}C NMR (100.6 MHz, C_6D_6, 298 K) of complex **2**.

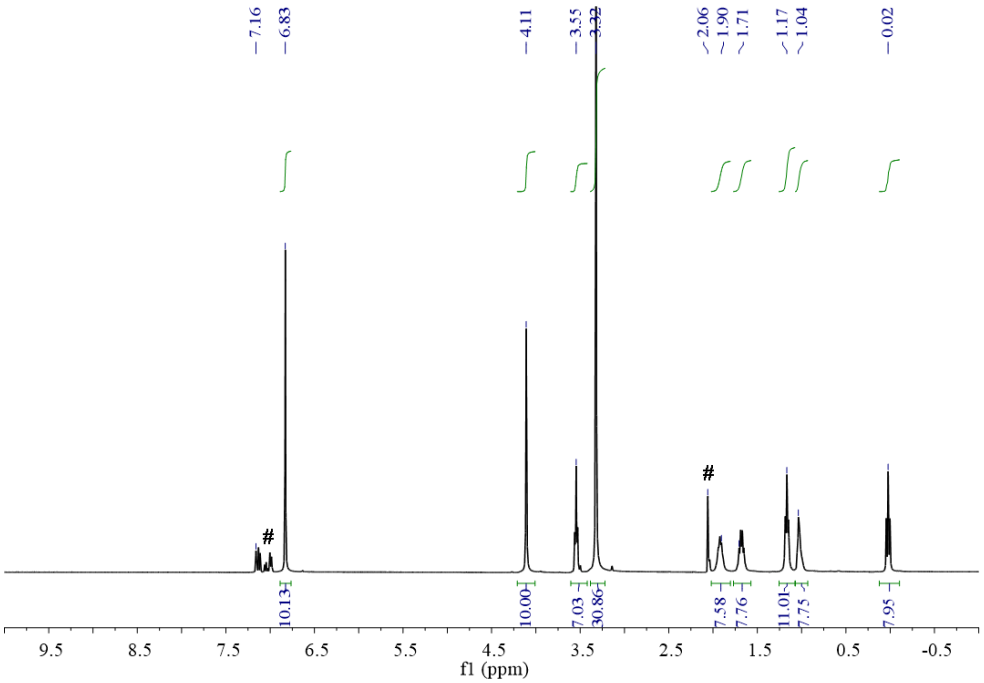

Fig. S17. ^{1}H NMR (400 MHz, C_6D_6, 298 K) of complex **3**. # represents toluene.

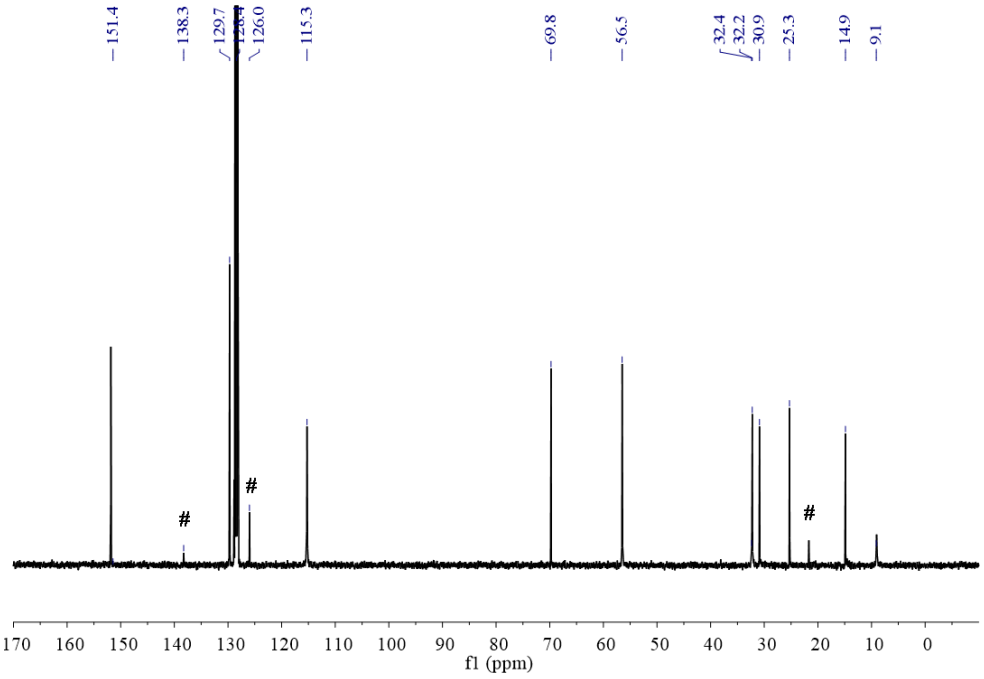

Fig. S18. ^{13}C NMR (100.6 MHz, C_6D_6, 298 K) of complex **3**. # represents toluene.

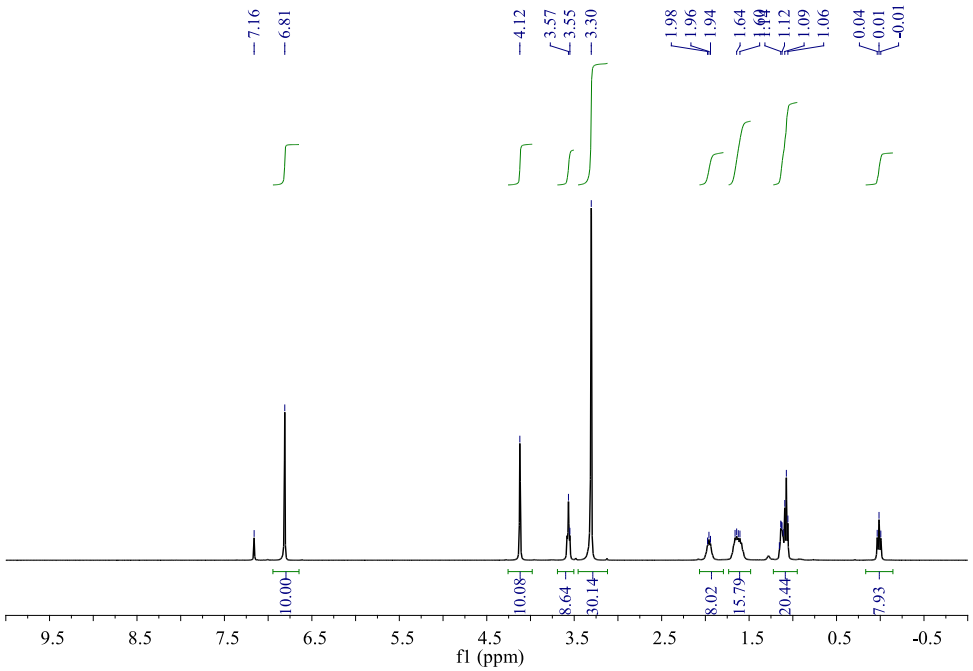

Fig. S19. ^{1}H NMR (400 MHz, C_6D_6, 298 K) of complex **4**.

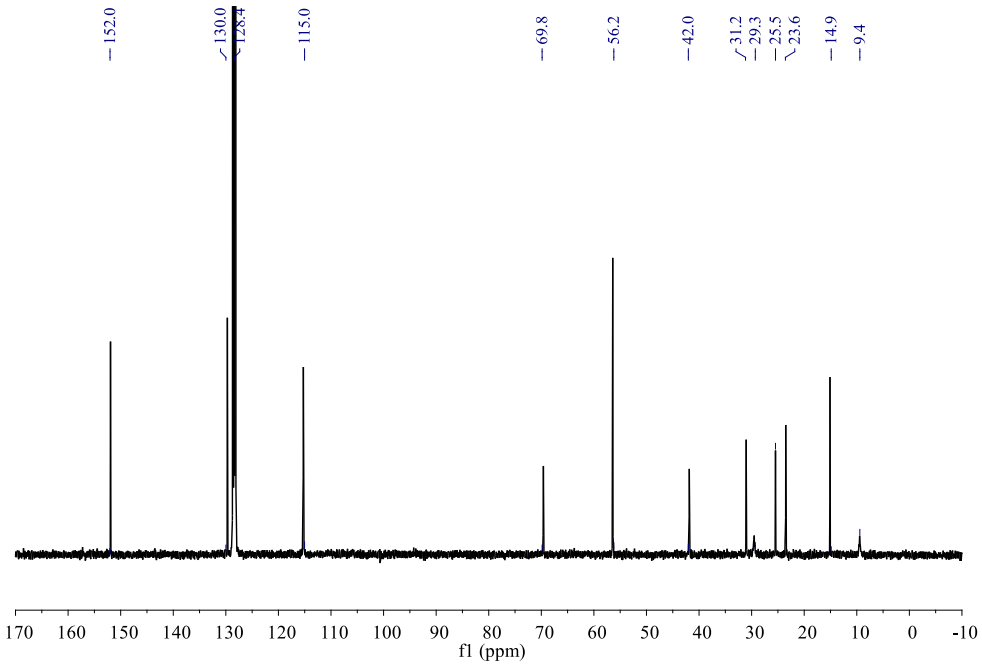

Fig. S20. ^{13}C NMR (100.6 MHz, C_6D_6, 298 K) of complex **4**.

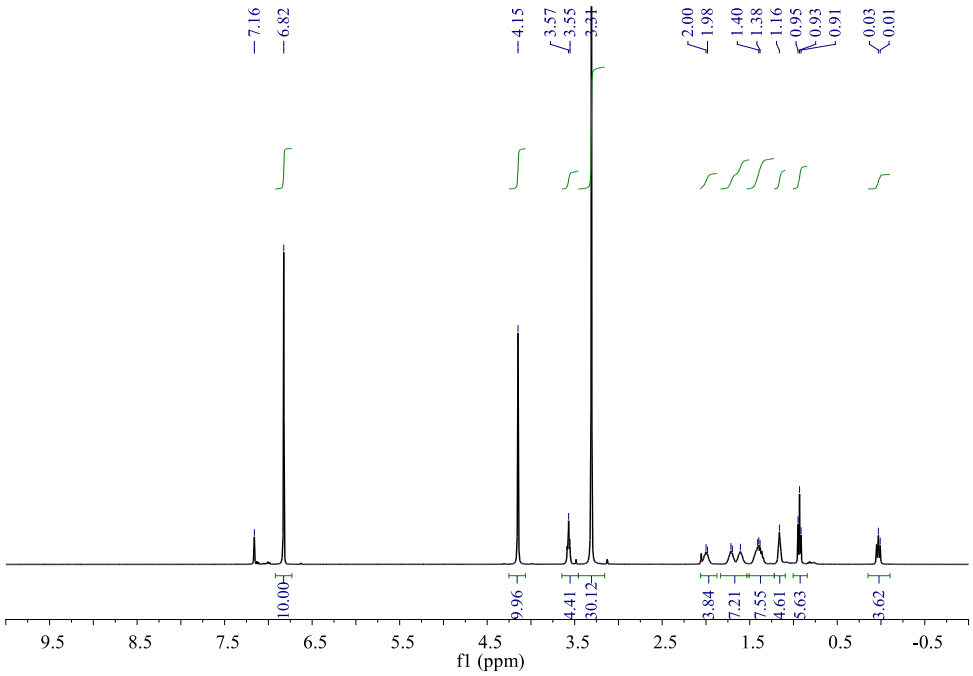

Fig. S21. ^{1}H NMR (400 MHz, C_6D_6, 298 K) of complex **5**.

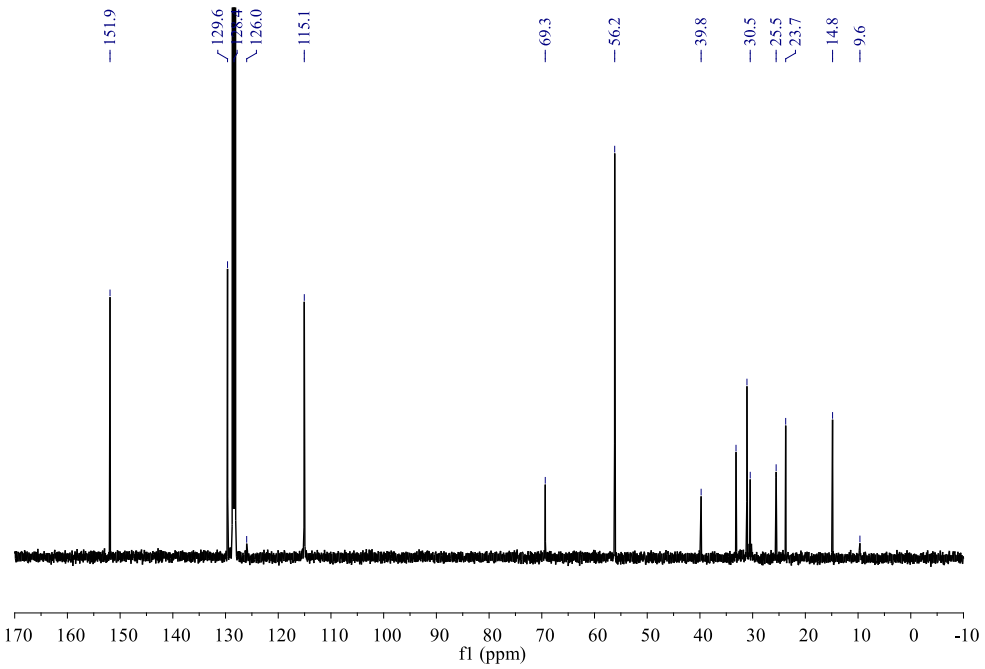

Fig. S22. ^{13}C NMR (100.6 MHz, C_6D_6, 298 K) of complex **5**.

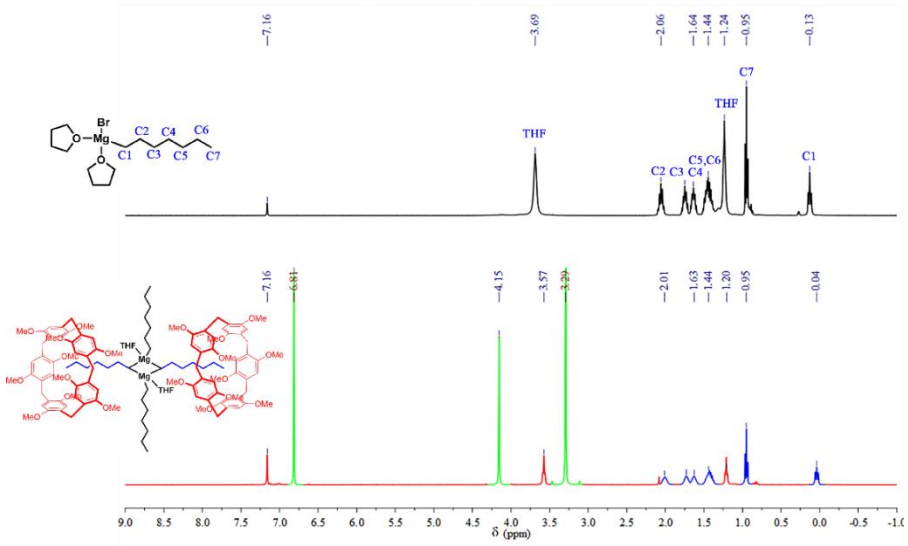

Fig. S23. ^{1}H NMR spectra (400 MHz, C_6D_6, 298 K) of (a) *n*-heptylmagnesium bromide; (b) Complex **5** (Green peaks are assigned to P5A, blue peaks to *n*-heptyl, and red peaks to solvents).

Table S3. Proton chemical shifts of the *n*-heptyl chain in complex **5** (in C_6D_6).

H	C1	C2	C3	C4	C5, C6	C7
Free	0.13	2.06	1.75	1.64	1.44	0.95
Complex	0.04	2.01	1.73	1.63	1.44	0.95
$\Delta\delta$	–0.09	–0.05	−0.02	−0.01	0	0

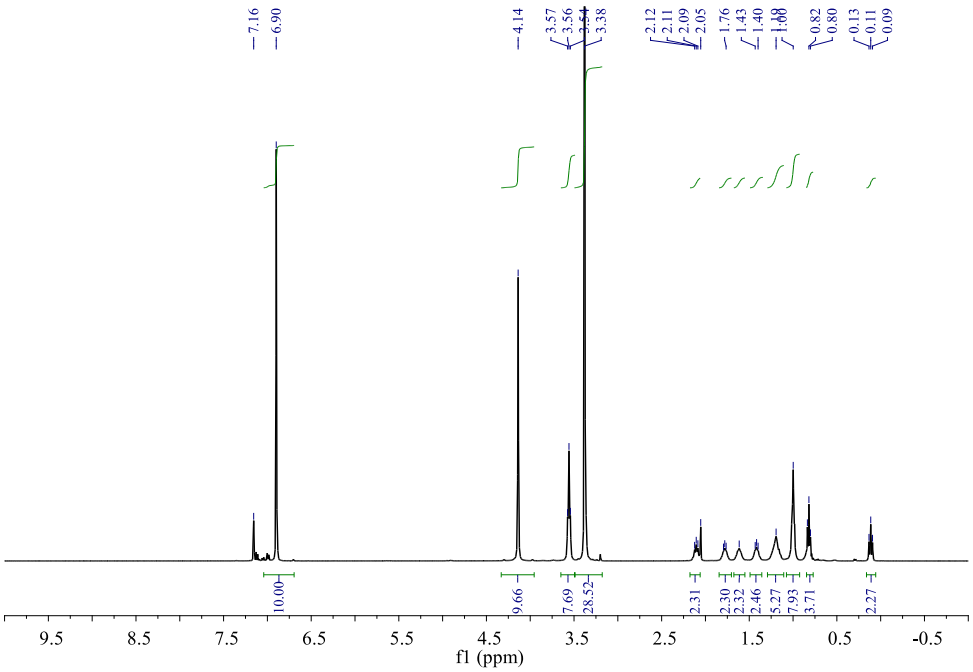

Fig. S24. ^{1}H NMR (400 MHz, C_6D_6, 298 K) of complex **6**.

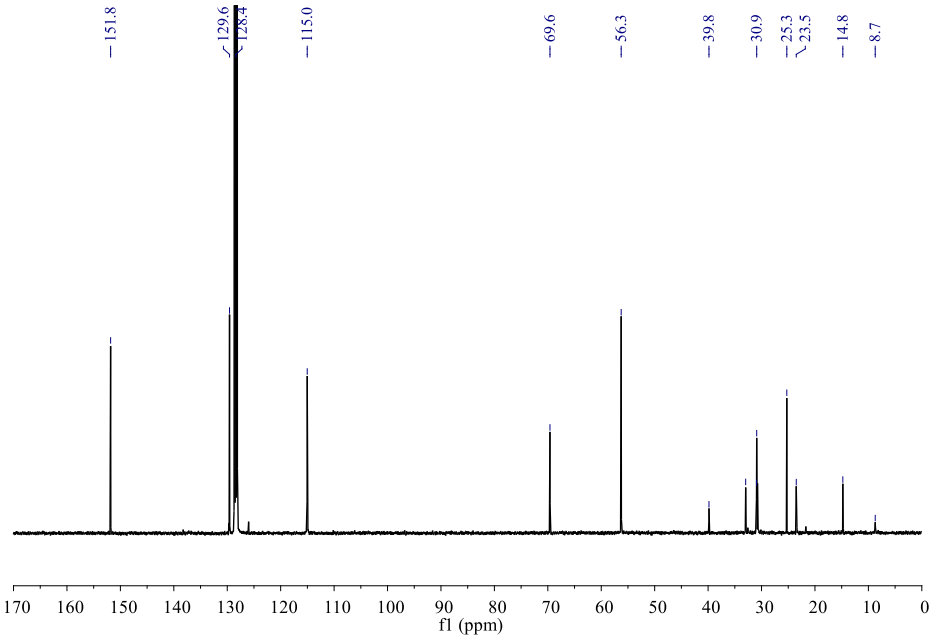

Fig. S25. ^{13}C NMR (100.6 MHz, C_6D_6, 298 K) of complex **6**.

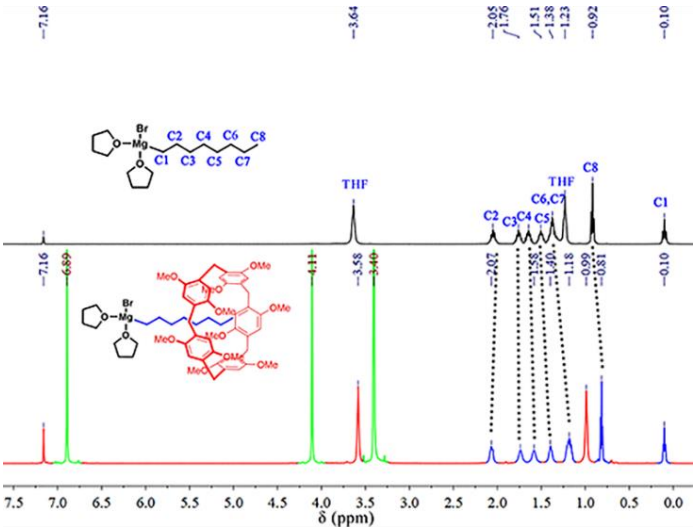

Fig. S26. ^{1}H NMR spectra (400 MHz, C_6D_6, 298 K) of (a) (*n*-octyl)MgBr(THF)$_2$ and (b) complex **6** (Green peaks are assigned to P5A, blue peaks to *n*-octyl, and red peaks to solvents).

Table S4. Proton chemical shifts of the *n*-octyl chain in complex **6** (in C_6D_6).

H	C1	C2	C3	C4	C5	C6, C7	C8
Free	0.10	2.05	1.76	1.65	1.51	1.38	0.92
Complex	0.10	2.07	1.74	1.58	1.40	1.18	0.81
$\Delta\delta$	0.00	0.02	−0.02	−0.07	−0.11	−0.20	−0.11

S4. DOSY studies of complexes 2, 5, 6

Diffusion-ordered ^{1}H NMR spectroscopy (DOSY) experiments were recorded on a Bruker Avance 600 spectrometer. The temperature was set and controlled at 298 K.

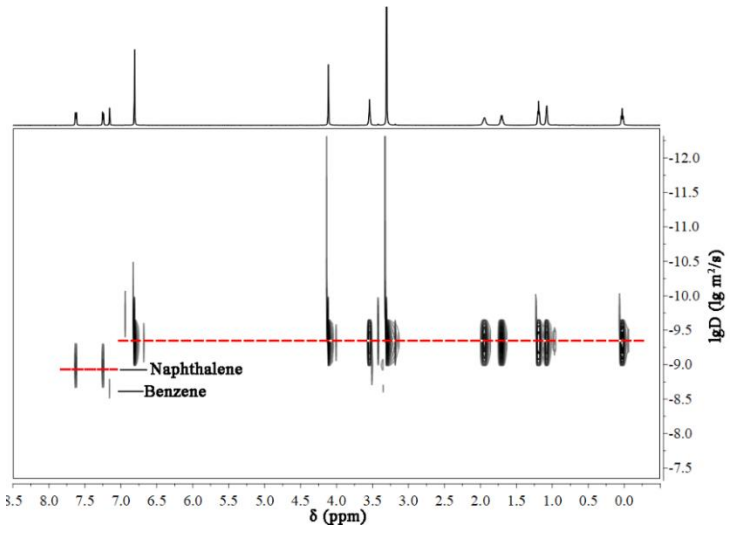

Fig. S27. DOSY spectrum (600 MHz, C_6D_6, 298 K) of complex **2**.

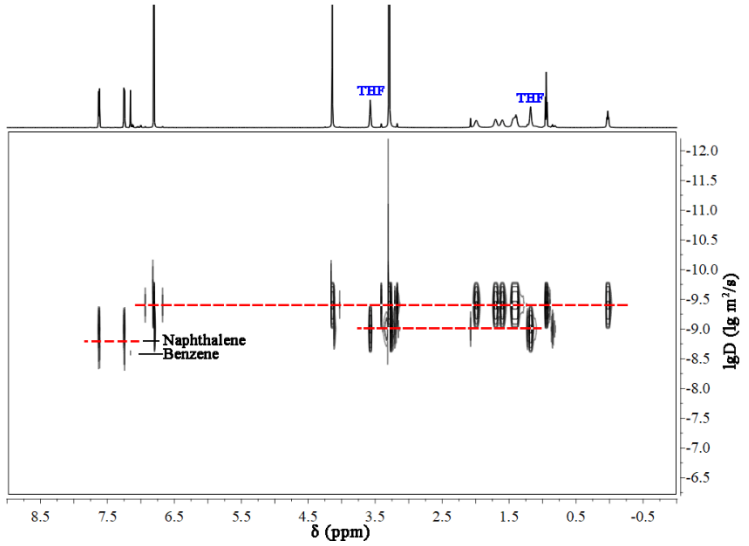

Fig. S28. DOSY spectrum (600 MHz, C_6D_6, 298 K) of **5**.

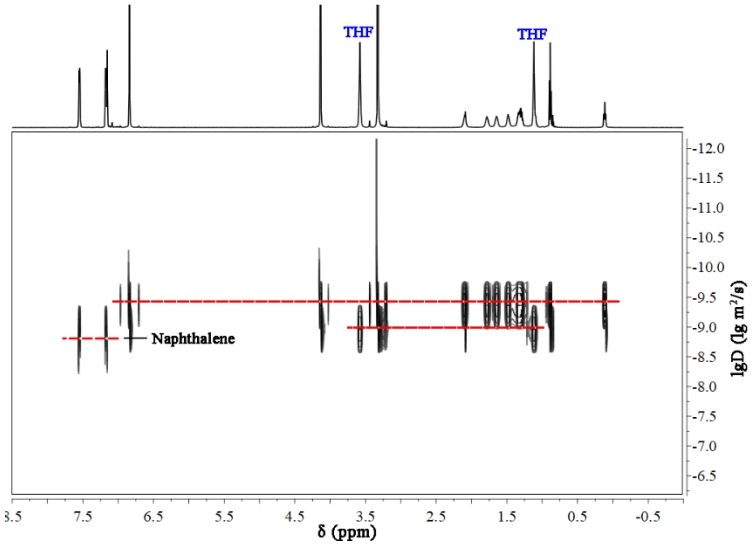

Fig. S29. DOSY spectrum (600 MHz, C_6D_6, 298 K) of **6**.

Diffusion coefficients and hydrodynamic radii are correlated theoretically by the Stokes-Einstein Relation (**Equation S1**):

$$\textbf{(S1)} \quad r = \frac{kT}{6\pi\eta D}$$

where D is the diffusion coefficient (obtained from Figs. S27–S29), k is the Boltzmann constant 1.3807×10^{-23} m^2 kg s^{-2} K^{-1}), T is the temperature in Kelvin (298 K), η is the viscosity of the solvent (benzene 6.36×10^{-4} kg m^{-1} s^{-1}), and r is the radius of the molecular sphere.

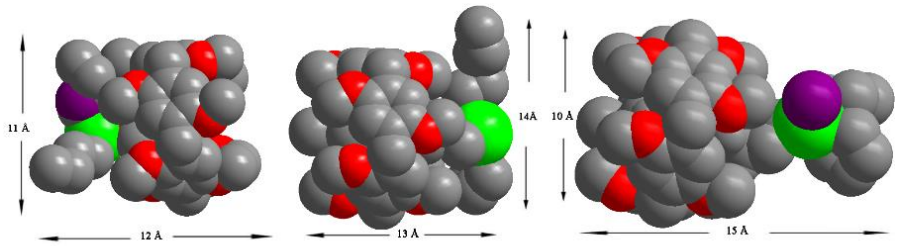

Fig. S30. Space filling models of complexes **2**, **5** and **6** showing their sizes.

Table S5. The hydrodynamic radius calculated from the DOSY experiments

Complex	D_x [m^2/s]	r (Å)
2	$4.623*10^{-10}$	7.4
5	$4.018*10^{-10}$	8.5
6	$3.990*10^{-10}$	8.6

Calculation of the molecular weights (MWs)

For molecular weight estimation, Stalke's method was applied with external calibration curves ECC's under merge parameters (because of the non-defined molecular shapes of the complexes in solution) using naphthalene (Naph) as internal reference with normalized diffusion coefficients. [12]

$$(\mathbf{S2})\ \log D_{\text{x.norm}} = \log D_{\text{ref.fix}} - \log D_{\text{ref}} + \log D_{\text{x}}$$

where $D_{\text{ref.fix}}$ is the fixed diffusion coefficient of the reference, D_{ref} is the measured diffusion coefficient of the reference, D_{x} is the diffusion coefficient of analyte x and $D_{\text{x.norm}}$ the relative diffusion coefficient of the analyte x normalized to the reference. In this article we used naphthalene (Naph.) as internal reference with the fixed diffusion coefficient:[12b]

$$(\mathbf{S3})\ \log D_{\text{ref.fix}}(\text{Naph.}) = -8.7650$$

To calculate the normalized diffusion coefficient ($D_{\text{x.norm}}$) of the analyte, naphthalene was added to the NMR sample and the diffusion coefficients of Naph. ($\log D_{\text{ref}}$) and the analyte ($\log D_{\text{x}}$) were measured and applied to **equation** (**S2**).

With equation (**S4**) it is possible to calculate the MWs.

$$(\mathbf{S4})\ \ MW\det = 10^{\left(\frac{\log D\text{x.norm} - \log K}{\alpha}\right)}$$

Table S6. Linear fit parameters for ECC_S in C_6D_6 solution.

	C_6D_6	
	$\log K$	α
$ECC^{C_6D_6}_{Merge}$	−7.58	0.572

Table S7. DOSY parameters for complexes **2, 5, 6.**

Complex	Formula (Main Species)	lgD_x [m^2/s]	lgD_{ref} [m^2/s]	MW(ECC) [g/mol]	MW(calc.) [g/mol]
2	$C_{56.28}H_{74.38}Br_{0.18}MgO_{11}$	–9.335	–8.835	891	966
5	$C_{59}H_{80}MgO_{10}$ (without [THF])	–9.395	–8.891	902	974
6	$C_{53}H_{64}BrMgO_{10}$ (without [THF])	–9.3990	–8.880	912	965

The results indicate that the size (Table S5) and molecular weight (Table S7) of complex **2** are close to a monomer in solution rather than a dimer as in the crystal structure. Moreover, the solvent THF molecules in complexes **5** and **6** show a slightly different diffusion coefficient from the host-guest system of pillar[5]arene with alkyl chain, but the THF molecules diffuse more slowly than benzene or even naphthalene (see Fig. S28 and S29), suggesting they are loosely bound to Mg or under fast association/dissociation in solution. The molecular weight of complex **5** (with heptyl chain) also corresponds to monomeric dialkyl magnesium (without THF) with pillar[5]arene, while that of **6** (with octyl chain) indicates the absence of two coordinating THF molecules. Thus, it appears that the dimerized Grignards seen in the solid state are dissociated to monomer in solution.

Reaction of encapsulated Grignard reagents (complex 6) with 3-pentanone

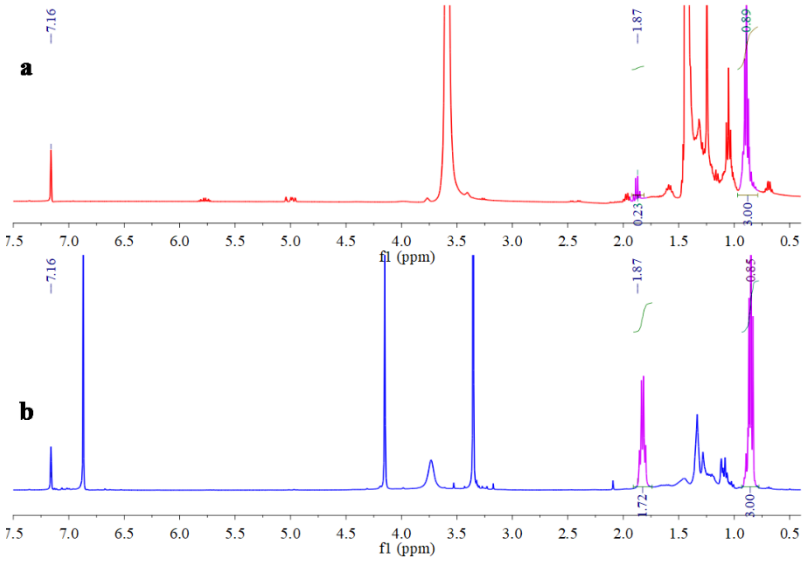

Fig. S31. Comparison of the ^{1}H NMR spectra (C_6D_6, 400 MHz, 298 K) of reactions (the peaks in purple mean 3-pentanone and the peak of 0.89 ppm also contains product). Reaction **a**: 100 μL of 1.0 M THF solution of *n*-octyl magnesium bromide was mixed with 3-pentanone (0.1 mmol) in 1 mL C_6D_6 at 6 ℃ for about 20 minutes. Reaction **b**: complex **6** (0.112 g, 0.1 mmol) was dissolved in 1 mL C_6D_6 and then 3-pentanone (0.1 mmol) was added at 6 ℃ for about 20 minutes.

As shown in Fig. S31, the reaction of 3-pentanone with free C_8MgBr proceeded rapidly even at low temperature (6 ℃; to avoid freezing of benzene) and almost finished in about 20 minutes. In contrast, the same reaction with **6** was much slower, thus suggesting the inclusion complex (**6**) may provide a possibility for the reaction to proceed in a controllable way.

S5. Supplemental References

1. K. Wang, L.-L. Tan, D.-X. Chen, N. Song, G. Xi, S. X.-A. Zhang, C. Li and Y.-W. Yang, *Org. Biomol. Chem.*, 2012, **10**, 9405-9409.
2. H. Y., T. Suezawa, M. Hirota, H. Takahashi, Y. Umezawa, K. Honda, S. Tsuboyama and M. Nishio, *J. Chem. Soc., Perkin Trans*. 2001, **2**, 2053–2058.
3. K. Jie, M. Liu, Y. Zhou, M. A. Little, S. Bonakala, S. Y. Chong, A. Stephenson, L. Chen and F. Huang, *J. Am. Chem. Soc*., 2017, **139**, 2908−2911.
4. A. Bondi, *Phys. Chem*., 1964, **68**, 441−451.
5. V. P. Colquhoun, B. C. Abele and C. Strohmann, *Organometallics*, 2011, **30**, 5408-5414.
6. A. R. Kennedy, R. E. Mulvey and S. D. Robertson, *Dalton Trans*., 2010, **39**, 9091−9099.
7. J. Intemann, J. Spielmann, P. Sirsch and S. Harder, *Chem. Eur. J*., 2013, **19**, 8478−8489.
8. G. M. Sheldrick, Program SADABS: Area-Detector Absorption Correction, University of Göttingen, Germany. 1996.
9. G. M. Sheldrick, *Acta Crystallogr., Sect. C: Cryst. Struct. Commun*. 2015, **71**, 3–8.
10. O. V. Dolomanov, L. J. Bourhis, R. J. Gildea, J. A. K. Howard and H. *J*. Puschmann, *Appl. Cryst.*, 2009, **42**, 339–341.
11. A. L. Spek, *Acta Cryst.*, 2015, **C71**, 9–18.
12. (a). R. Neufeld and D. Stalke. *Chem. Sci*. 2015, **6**, 3354–3364. (b). S. Bachmann, R. Neufeld, M. Dzemski and D. Stalke, *Chem. Eur. J*. 2016, **22**, 8462–8465.